Loss of the nodule-specific cysteine rich peptide, NCR169, abolishes symbiotic nitrogen fixation in the *Medicago truncatula dnf7* mutant

Beatrix Horváth[a], Ágota Domonkos[a], Attila Kereszt[b], Attila Szűcs[b], Edit Ábrahám[b], Ferhan Ayaydin[c], Károly Bóka[d], Yuhui Chen[e], Rujin Chen[e], Jeremy D. Murray[e,f], Michael K. Udvardi[e], Éva Kondorosi[b], and Péter Kaló[a,1]

[a]National Agricultural Research and Innovation Centre, Agricultural Biotechnology Institute, Gödöllő 2100, Hungary; [b]Institute of Biochemistry, Biological Research Center, Szeged 6726, Hungary; [c]Cellular Imaging Laboratory, Biological Research Center, Szeged 6726, Hungary; [d]Department of Plant Anatomy, Eötvös Loránd University, Budapest 1117, Hungary; [e]Plant Biology Division, The Samuel Roberts Noble Foundation, Ardmore, OK 73401; and [f]Department of Cell and Developmental Biology, John Innes Centre, Norwich NR4 7UH, United Kingdom

Edited by Frederick M. Ausubel, Harvard Medical School, Massachusetts General Hospital, Boston, MA, and approved July 9, 2015 (received for review January 18, 2015)

Host compatible rhizobia induce the formation of legume root nodules, symbiotic organs within which intracellular bacteria are present in plant-derived membrane compartments termed symbiosomes. In *Medicago truncatula* nodules, the *Sinorhizobium* microsymbionts undergo an irreversible differentiation process leading to the development of elongated polyploid noncultivable nitrogen fixing bacteroids that convert atmospheric dinitrogen into ammonia. This terminal differentiation is directed by the host plant and involves hundreds of nodule specific cysteine-rich peptides (NCRs). Except for certain in vitro activities of cationic peptides, the functional roles of individual NCR peptides in planta are not known. In this study, we demonstrate that the inability of *M. truncatula dnf7* mutants to fix nitrogen is due to inactivation of a single NCR peptide, NCR169. In the absence of NCR169, bacterial differentiation was impaired and was associated with early senescence of the symbiotic cells. Introduction of the *NCR169* gene into the *dnf7-2/NCR169* deletion mutant restored symbiotic nitrogen fixation. Replacement of any of the cysteine residues in the NCR169 peptide with serine rendered it incapable of complementation, demonstrating an absolute requirement for all cysteines in planta. *NCR169* was induced in the cell layers in which bacteroid elongation was most pronounced, and high expression persisted throughout the nitrogen-fixing nodule zone. Our results provide evidence for an essential role of NCR169 in the differentiation and persistence of nitrogen fixing bacteroids in *M. truncatula*.

Sinorhizobium | ineffective nodules | symbiotic host peptides | senescence | bacteroid differentiation

Legumes form endosymbiotic interactions with nitrogen-fixing soil bacteria, called rhizobia. In these symbioses, the plant provides a microaerobic environment and energy source for bacterial nitrogen fixation, and in return receives fixed nitrogen in the form of ammonium (1). Following mutual recognition, regulated developmental programs are induced in both partners leading to the formation of root nodules (2). In root hairs, host compatible rhizobia initiate the development of infection threads, along which the bacteria grow. In parallel, mitosis of cortical and pericycle cells is induced, and their proliferation leads to the formation of the nodule primordium. The infection threads grow down through the cortex and when they reach the nodule primordia, rhizobia are released and colonize nodule cells via endocytosis. Within the infected nodule cells, bacteria are surrounded by the plant-derived peribacteroid membrane, which delimits a new, facultative nitrogen-fixing organelle called the symbiosome. During nodule development, infected nodule cells also undergo differentiation; they become polyploid via multiple rounds of endoreduplication, which results in enlargement of cells that eventually become packed with thousands of symbiosomes (3, 4).

Sinorhizobium (*Ensifer*) *meliloti* and *S. medicae* establish symbioses with *Medicago truncatula* leading to the formation of indeterminate nodules. This nodule type is characterized by a persistent nodule meristem and a gradient of cells in different developmental states forming specific histological zonation (5). Continuous cell proliferation in the meristem (zone I) produces cells that exit the mitotic cycle and enter cell differentiation. Zone II corresponds to the infection zone where bacteria are released from the infection threads and then these infected symbiotic cells undergo gradual differentiation. Growing, infected plant cells host more and more multiplying symbiosomes. Eventually, symbiosome proliferation ceases in older cells of Zone II, although replication of bacterial genomes continues without cell division, resulting in enlarged/elongated polyploid bacteroids. Some of the most striking changes occur in the interzone (zone II-III), a transition zone characterized by amyloplast deposition. In this zone, both rhizobia and symbiotic nodule cells complete their differentiation with the last rounds of endoreduplication and final enlargement of cells. The nitrogen-fixing zone III comprises the major part of a functional nodule wherein the differentiated bacteroids reduce atmospheric nitrogen. The developmental switches of symbiotic nodule cells are accompanied by altered size, shape and appearance of the vacuoles, which become larger in the older Zone II cells, collapse in the transition zone, and then reappear in mature nitrogen fixing cells (6). As nodule cells age, nitrogen-fixation ceases and degradation of these cells leads

Significance

In certain legume–rhizobia symbioses, the host plant is thought to control the terminal differentiation of its bacterial partner leading to nitrogen fixation. In *Medicago truncatula*, over 600 genes coding for nodule-specific cysteine-rich (NCR) peptides are expressed during nodule development and have been implicated in bacteroid differentiation. Up to now it was generally assumed that most of these peptides, if not all, act redundantly. By demonstrating that deletion of a single member of the *NCR* gene family can result in an ineffective symbiotic phenotype, we show that specific NCR peptides can have essential, nonredundant roles in controlling bacterial differentiation and symbiotic nitrogen fixation.

Author contributions: A.K., R.C., M.K.U., É.K., and P.K. designed research; B.H., Á.D., E.Á., F.A., K.B., Y.C., and J.D.M. performed research; A.K., A.S., É.K., and P.K. analyzed data; and A.K., M.K.U., É.K., and P.K. wrote the paper.

The authors declare no conflict of interest.

This article is a PNAS Direct Submission.

Data deposition: The data reported in this paper have been deposited in the Gene Expression Omnibus (GEO) database, www.ncbi.nlm.nih.gov/geo (accession no. GSE65328).

[1]To whom correspondence should be addressed. Email: kalo@abc.hu.

This article contains supporting information online at www.pnas.org/lookup/suppl/doi:10.1073/pnas.1500777112/-/DCSupplemental.

to formation of the senescence zone (zone IV), proximal to the root, where bacteroids are digested.

The differentiation of the endosymbionts is irreversible as they are unable to resume cell proliferation and to reenter the free-living life-style (7). *M. truncatula* and other IRLC (Inverted Repeat-Lacking Clade) legumes possess a remarkably large number of genes encoding nodule-specific cysteine-rich (NCR) peptides (8–12). The genome of *M. truncatula* contains more than 600 *NCR* genes (13). The peptides enter the secretory pathway and the relatively conserved signal peptides are cleaved off by the signal peptidase complex in the endoplasmic reticulum (14). The mature peptides are composed of 30–50 amino acids and differ in composition and sequence, except for conserved positions of four or six cysteine residues (15). At least 138 NCR peptides are known to be targeted to the symbiosomes (16–18) and failure of their delivery to the symbiosomes impairs bacteroid differentiation in *M. truncatula* (16). The functions of individual NCRs as well as their combined action have remained elusive until now. Their expression at different stages of symbiotic cell development suggests distinct roles for members of this family. NCRs resemble defensin-type antimicrobial peptides in some ways. Several cationic NCR peptides display in vitro antimicrobial (bactericide and fungicide) activities (19, 20). Such NCRs expressed in the older cells of Zone II could contribute to the arrest of proliferation of bacteroids. Chemically synthesized NCR247 interacts with multiple proteins in vitro and such interactions might affect different aspects of bacteroid physiology, including gene expression, translation and arrest of cell division (17, 21). A question is whether NCR peptides function collectively or whether individual peptides might fulfill unique and essential roles. In this study, we found that loss of the *NCR169* gene in the *M. truncatula* deletion mutant *dnf7* (defective in nitrogen fixation) impairs symbiotic nitrogen-fixation. We show that the *NCR169* gene fully restores the wild-type (WT) symbiotic phenotype of the *dnf7* mutant and demonstrate that the in planta biological activity requires all of the cysteine residues of NCR169. In *dnf7* mutant nodules, bacteroid differentiation was incomplete, although late nodulin genes and the bacterial *nifA* regulated genes required for the nitrogenase enzyme complex assembly were expressed. The mutant phenotype indicates that *NCR169* is required for complete differentiation of bacteroids and their persistence in *M. truncatula* nodules.

Results

***DNF7* Is Required for the Development and Persistence of Nitrogen Fixing Bacteroids.** The nitrogen fixation mutant *dnf7-2* was identified in a genetic screen of a fast-neutron-bombarded population of *M. truncatula* cv. Jemalong (22). The *dnf7-2* mutant showed symptoms of nitrogen starvation under symbiotic conditions (Fig. S1 *A* and *B*) and developed white slightly cylindrical nodules following inoculation with *S. meliloti*.

To test the rhizobial strain dependence of the *dnf7-2* mutant phenotype, WT and *dnf7-2* plants were inoculated with *S. meliloti* 1021 and a more effective symbiotic partner, *S. medicae* WSM419 (23), both constitutively expressing the *lacZ* reporter gene. Longitudinal sections of nodules 3 wk post inoculation (wpi) were stained for β-galactosidase activity and analyzed by light microscopy. Wild-type nodules induced by either strain showed the characteristic zonation and predominant staining in the mature symbiotic cells completely filled with bacteroids (Fig. 1 *A* and *B*). The symbiotic phenotype of *dnf7-2* nodules was the same with each rhizobial strain; there were decreased numbers of symbiotic cells and no β-galactosidase staining in the region corresponding to Zone III (Fig. 1 *C* and *D*). Nodule cell structure and endosymbiont morphology were further analyzed with SYTO13-staining of nodule sections. Bacterial release and development of symbiotic cells in the infection zone of WT and mutant nodules were similar, including enlargement of the vacuoles in the older zone II cells (Fig. 1 *E* and *H* and Fig. S1 *C* and *F*). In WT and *dnf7-2* nodules induced by *S. medicae* WSM419, shrinking and disappearance of the vacuoles was observed in the transition zone (Fig. 1 *F* and *I*), but this was less apparent in nodules infected with *S. meliloti* 1021 (Fig. S1 *D* and *G*). In WT nodules, elongated nitrogen-fixing bacteria were orientated toward the vacuoles (Fig. 1*G* and Fig. S1*E*). By contrast, in comparable cells of mutant nodules, the bacteroids were shorter (Fig. 3*G*) and disorganized and in addition vacuole development was also somewhat impaired (Fig. 1*J* and Fig. S1*H*).

Amyloplast accumulation is characteristic for the transition zone. Staining of nodule sections with potassium iodide revealed similar extents of amyloplast deposition in the transition zone of both the WT and mutant nodules (Fig. 1 *K–N*). In WT and *dnf7-2* nodules induced by *S. meliloti* 1021, the presence of amyloplasts in zone III or in the corresponding region of mutant nodules and the less apparent vacuole transition in the symbiotic cells might correlate with the less effective symbiotic partnership between *M. truncatula* cv. Jemalong and *S. meliloti* 1021 (23).

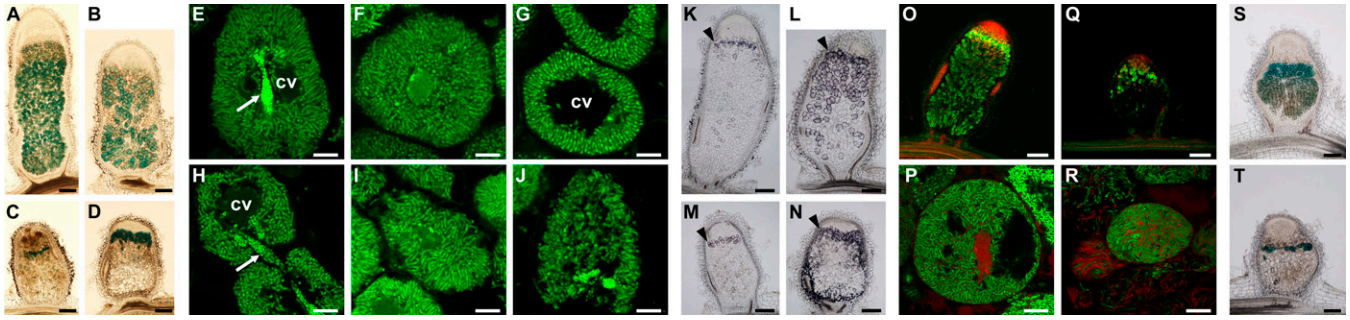

Fig. 1. Symbiotic cells do not persist in the nitrogen fixation zone of *dnf7-2* nodules. β-galactosidase activity was detected histochemically in sections of wild-type (WT) (*A* and *B*) and mutant (*C* and *D*) nodules induced by *S. medicae* WSM419 (*A* and *C*) or *S. meliloti* 1021 (*B* and *D*) strains harboring the constitutive *lacZ* reporter gene. Confocal images of SYTO13-stained WT (*E–G*) and *dnf7-2* (*H-J*) nodule sections induced by *S. medicae* show similar changes in vacuole volume in the infection (*E* and *H*) and transition zones (*F* and *I*) while in the mutant the vacuoles are less developed and the symbiosomes are more disorganized in the distal Zone III cell layers (*J*) compared with WT cells (*G*). Starch accumulated in the transition zones of 3-wk-old WT (*K* and *L*) and mutant nodules (*M* and *N*) induced with *S. medicae* WSM419 (*K* and *M*) and *S. meliloti* 1021 (*L* and *N*). Live/dead staining revealed fewer infected host cells in zone III of *dnf7-2* nodules (*Q*) compared with WT (*O*). In contrast with the presence of living bacteria in WT nodules (*P*), a mixture of live and dead rhizobia exists in the mutant nodules (*R*). Wild-type and *dnf7-2* plants were inoculated with *S. meliloti* 1021 carrying the P*nifH::GUS* reporter fusion revealing *nifH* expression in the entire nitrogen-fixation zone of WT nodules (*S*) but in *dnf7-2* nodules its expression was limited to the cells of the transition zone (*T*). Arrow: infection thread with nonreleased bacteria. Arrowheads: KI-stained amyloplasts containing starch granules in the transition zone. cv: central vacuole. (Scale bars: 200 μm in *A–D*, *K–O*, *Q*, *S*, and *T* and 10 μm in *E–J*, *P*, and *R*.)

The viability of *S. meliloti* and *S. medicae* was investigated by live and dead staining of nodule sections with the fluorescent nucleic acid dyes, SYTO9 and propidium iodide (PI). SYTO9 stains living bacteria green, whereas cells with damaged membranes take up PI and exhibit internal red fluorescence. Three wpi, living green fluorescent bacteria were present in all zones of WT nodules (Fig. 1*O* and Fig. S1*J*). In the *dnf7-2* nodules, live bacteria were seen in zone II and in the transition zone (Fig. 1*Q* and Fig. S1*L*); however in the few infected cells present in the region corresponding to Zone III (Fig. 1*Q* and Fig. S1*L*), living and dead or dying bacteria coexisted (Fig. 1*R* and Fig. S1*M*). In contrast, in WT nodules all bacteroids were viable/green (Fig. 1*P* and Fig. S1*K*).

A previous study found that nitrogenase was inactive in *dnf7* mutant nodules 18 d post inoculation (dpi) (22). To determine whether the *nifH* gene, coding for a subunit of the nitrogenase complex was expressed in the mutant, WT and *dnf7-2* plants were inoculated with *S. meliloti* 1021 strain carrying the *nifH* promoter-GUS reporter gene fusion (P*nifH::uidA*) (24). The *nifH* promoter was found to be active in both WT and *dnf7-2* nodules, but unlike the WT nodules where expression was found both in the transition zone and throughout the mature nitrogen fixation zone (Fig. 1*S*), at 14 dpi, *nifH* promoter activity in the mutant was limited to a belt of a few cells (Fig. 1*T*). This observation indicates that although the bacterial *nifH* gene could be induced in *dnf7-2* nodules, its expression was restricted and apparently insufficient for substantial nitrogen fixation (22, 24).

The Gene *Medtr7g029760* Is Deleted in Multiple *dnf7* Alleles. Genetic mapping identified the position of the *dnf7-2* locus on the upper arm of chromosome 7 between genetic markers MtbB183 and h2_5f17a (www.medicago.org) using a mapping population consisting of 565 F2 plants (Fig. S2*A*). Parallel to the genetic mapping, a microarray-based cloning approach, which was successfully used previously to clone the *VPY* gene in *M. truncatula* (25), was applied to identify the *DNF7* gene. Genomic DNA of *dnf7-2* and WT plants was hybridized to Affymetrix Medicago GeneChips and comparison of mutant and WT hybridization signals of individual probe sets revealed four putative genomic DNA deletions in *dnf7-2* (Fig. S2*B*). The genomic location of the probe set showing the lowest mutant/WT hybridization signal ratio coincided with the map position of the symbiotic phenotype, linking this putative deletion and the ineffective phenotype (Fig. S2*B*). To verify this link, we made use of the previously described allele *dnf7-1* (24) and two other alleles from this study, *dnf7-3 and dnf7-4* (represented by mutants FN839-2 and FN9233). PCR-based markers were used to define overlapping deletions of about 55 kb, 85 kb, and at least 190 kb in these mutants (Figs. S2*C* and S3). The analysis of the gene content in the smallest deleted region identified two genes, Medtr7g029850, encoding a hypothetical protein, Medtr7g029760 corresponding to an *NCR* gene (Table S1*B*) and several transposable element-related gene models (Mt4.0 JBrowse, ref. 26). Analysis of the expression profile of the two genes in the *M. truncatula* Gene Expression Atlas (27) revealed that the gene corresponding to Medtr7g029760 has a nodule-specific expression pattern, suggesting it could be *DNF7*.

NCR169 Is Required for an Effective Symbiosis with *Sinorhizobium* Species and its Cysteine Residues Are Essential for the Symbiosis. The NCR169 peptide encoded by *Medtr7g029760* is a member of the large nodule-specific cysteine-rich peptide family. The gene encodes a predicted protein containing a 23-aa signal peptide (28) preceding a mature peptide of 38 amino acids, that is slightly cationic (pI = 8.45) and contains 4 cysteines in conserved positions (Fig. S2*D*). We confirmed that the loss of this gene caused the ineffective symbiotic phenotype by transforming the *dnf7-2* mutant with the *NCR169* gene together with 1,178 bp 5′ to the translation start site. This transformation resulted in normal nodule development and nitrogen fixation (Fig. 2*B*) and so *DNF7* was renamed *NCR169*.

To investigate whether the *NCR169* gene is conserved in legumes that impose terminal bacteroid differentiation on their symbiotic partners, homologous sequences were sought in the publicly available BioProject data sets of *Medicago sativa* (SRX375984-375988), *Melilotus albus* (SRX684712, SRX686657), *Trifolium pratense* (PRJNA257076), and the transcriptome of *Pisum sativum* (PRJNA257308). Peptides that were identical or very similar to NCR169 (68% sequence identity in the mature peptide) were found in the genomes of *M. sativa* and *M. albus* (Fig. S2*E*), but not in *T. pratense* or *P. sativum*.

Disulfide bridges play an important role in the folding and stability of secreted peptides/proteins. Replacement of cysteine residues with serine was shown to reduce but not to abolish the in vitro antimicrobial activity of the NCR247 peptide (29). To test whether the cysteine residues of NCR169 are required for its activity in planta, we generated constructs coding for modified NCR169 peptides wherein single and multiple cysteine residues were substituted with serines. Neither single substitutions of each of the cysteine residues ($NCR169_{C32S,\ C38S,\ C51S,\ C56S}$) nor the double mutant ($NCR169_{C32S\text{-}C51S}$) were able to restore a functional symbiosis to the *dnf7-2* mutant, indicating an absolute requirement for each cysteine residue for the function of NCR169 (Fig. 2 *A–C* and Fig. S4 *A–Y*).

***NCR169* Is Expressed in Symbiotic Cells and the Peptide Localizes to the Symbiotic Compartment.** Expression of *NCR* genes is highly specific for nodules and they are almost exclusively active in the infected symbiotic cells (16, 30). To investigate the expression of *NCR169*, its promoter fused to the *uidA* reporter gene was introduced into WT *M. truncatula*, using *Agrobacterium rhizogenes*-mediated hairy-root transformation. *NCR169* expression was detected in infected cells in the transition and mature nitrogen-fixation zones (Fig. S5*B*). This expression pattern is in agreement with RNA-sequencing data from different nodule zones obtained by laser-capture microdissection (ref. 31 and Fig. S5*C*). To analyze the temporal induction of *NCR169*, we monitored its expression using quantitative RT-PCR (qRT-PCR) following inoculation

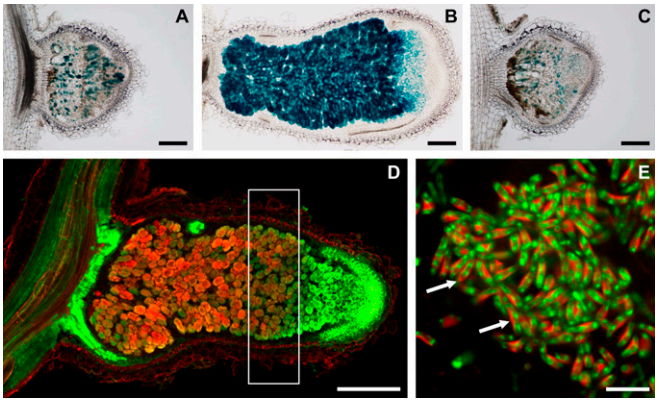

Fig. 2. Conserved cysteines of NCR169 are required for its function in planta (*A–C*) and a NCR169-mCherry fusion protein localizes to the symbiotic compartment (*D* and *E*). The empty vector control (*A*), the wild-type (*B*) and the C32S mutant *NCR169* gene (*C*) as well as the *NCR169-mCherry* (*D*) gene constructs were introduced into *dnf7-2* roots with *A. rhizogenes*-mediated hairy-root transformation. Nodules on *dnf7-2* roots transformed with the wild-type *NCR169* gene showed characteristic zonation indicating the restoration of the symbiotic phenotype (*B*). The substitution of each cysteine residue abolished complementation by the mutant *NCR169* genes indicating the essential role of its cysteines (*C* and Fig. S4). NCR169-mCherry fusion protein restored the symbiotic phenotype of *dnf7-2* (*D*) at 21 dpi. In the distal part of Zone III (white rectangle), the green fluorescence of SYTO13 staining of the bacteroids does not overlap with the red mCherry signal surrounding the bacteroids in the peribacteroid space (*E*). Arrows: the signal of NCR169-mCherry fusion proteins in the peribacteroid space. (Scale bars: 200 μm in *A–D* and 10 μm in *E*.)

with *S. medicae* WSM419. Low levels of expression were detected 7 and 10 dpi and a large increase in expression was found 14 dpi, followed by a slight decline 21 dpi (Fig. S5*D*).

Many NCR peptides are targeted to and copurify with bacteroids (16–18). To ascertain the localization of NCR169, the genomic sequence of the gene was fused in frame to the sequence encoding mCherry fluorescent protein and introduced into *dnf7-2* roots, using hairy-root transformation. The construct restored an effective symbiosis indicating that the fluorescent tag did not interfere with the normal activity of NCR169. The red signal of mCherry was observed in the nitrogen-fixation zone (Fig. 2*D*), consistent with the observed expression pattern of *NCR169*. The mCherry signal was adjacent to and largely separate from the green SYTO13 fluorescence of bacteroids (Fig. 2*E*).

Full Induction of Late Nodulin Genes Is Impaired in *dnf7* Nodules. To investigate how the lack of NCR169 affects the expression of other genes, the transcriptome of nodules 15 dpi was analyzed, by RNA sequencing of both the bacteroid and plant cells. This analysis confirmed that genes associated with the onset of nitrogen fixation (ref. 32 and Table S2) and considered as late nodulation markers, such as the bacterial *nif* and the plant *MtN31* (*NCR158*), *MtLB1*, and *MtCAM1* genes (33), were expressed in the *dnf7-2* nodules. However, of the plant genes induced during nodule development in WT plants (32), 35% were expressed at significantly lower levels in *dnf7-2* nodules, in agreement with the data of Mitra and Long (33). Furthermore several cysteine protease genes were induced in the mutant nodules, consistent with the initiation of early senescence (Fig. S6).

In the current release of the *M. truncatula* genome (v4.0), we identified 685 genes coding for NCR peptides. Of these, 383 showed significant (more than 100 reads per kilobase of gene model per million mapped reads) expression in the RNA sequencing data obtained from laser-capture microdissected nodule zones (31). Of these 383 *NCR* genes, 64 were expressed at lower levels in the *dnf7-2* mutant than in the WT, indicating that the expression of these NCR peptides is dependent on the proper function of NCR169. Based on the distribution of the sequence reads, the expression of these *NCR* genes in WT nodules is higher in Zone III than in the transition zone (31). In contrast, *NCR169* and *NCR* genes that did not show lower expression in *dnf7-2* had higher expression levels in the transition zone (Fig. S5*C*). We measured *NCR169* and *NCR211* transcript levels in 14 dpi nodules of *dnf4*, which is deficient in production of NCR211, and *dnf7-2* and compared them to those of the WT and the *sta1* developmental mutant, which produces fewer but effective nitrogen fixing nodules (34). *NCR169* and *NCR211* were expressed in *dnf4* and *dnf7-2*, respectively, but at lower levels than in the WT and the *sta1* mutant (Fig. S5*E*). The lower expression levels in the *dnf* mutant nodules correlated with reduced numbers of symbiotic cells, in line with a recent study demonstrating a correlation between the expression level of *NCR*s and rhizobial occupation of nodules (35).

Bacteroid Elongation Is Impaired in *dnf7-2* Nodules. To understand better the developmental defects caused by the absence of NCR169, the morphology of symbiotic cells was studied with transmission electron microscopy. This analysis revealed that bacterial cells in the transition zones of *dnf7-2* and WT nodules were comparable (Fig. 3 *A* and *D*). In contrast, older cells of *dnf7-2* nodules had a disorganized cellular structure in which bacteroids were atypical and electron dense (Fig. 3 *E* and *F*). These irregularly shaped bacteroids were not tightly surrounded by the peribacteroid membrane. Furthermore, there was aggregation of the host cytoplasm and the presence of small undifferentiated bacteria that are probably liberated from the infection threads during degradation of plant cells (Fig. 3*F*). All this indicates these cells were in an advanced stage of senescence.

To investigate how the deficiency in NCR169 affects bacterial elongation, a characteristic feature of terminal bacteroid differentiation, we measured and compared the length of rhizobia in the transition zone of WT and mutant nodules 21 dpi. A shift in the average size of bacteroids toward a lower value in the mutant compared with the WT was found (Fig. 3*G*). The bacterial population isolated from mutant nodules (Fig. 3*K*) showed reduced amplification of the genome compared with that of WT nodules (Fig. 3*J*), reflecting incomplete bacteroid differentiation. The lower DNA content and reduced bacterial cell elongation indicate that NCR169 is required for the complete differentiation of bacteroids; probably the failure of differentiation induces the degradation of bacteroids. Consistent with the incomplete bacteroid differentiation, a lower proportion of plant cells was present at high ploidy level (16C – 64C) in mutant nodules than in WT indicating incomplete maturation of symbiotic cells (Fig. 3 *H* and *I*).

Loss of NCR169 Function Triggers Early Senescence. The brown pigmentation in *dnf7-2* nodules (Fig. 1 *C* and *D*) as well as the greenish-blue coloration observed after toluidine-blue staining (Fig. S6*C*) indicates the presence of polyphenolic compounds, which are often associated with defense reactions and/or senescence. Polyphenol accumulation was more widespread in older (6 wpi) cells of *dnf7-2* nodules (Fig. S6 *D* and *E*). The transcriptional activation of genes annotated as senescence and defense-related genes was measured 14 dpi using RNA-sequencing and the expression of representative genes was analyzed by qRT-PCR. Cysteine proteinase genes associated with senescence in *M. truncatula* (36) were highly up-regulated in the *dnf7-2* and *dnf4* mutants, whereas in WT and *sta-1* mutant plants, these genes were not induced (Fig. S6*A*). In addition, genes associated with pathogenic responses, such as the *NDR1* (a Non-race-specific Disease Resistance) and a chitinase gene were not induced in *dnf7-2* and *dnf4* mutants, indicating that the defense-like reactions in mutant nodules are provoked by developmental senescence rather than defense signaling networks.

Discussion

In this study, NCR169, one of over 600 nodule-specific NCR peptides, was shown to be essential for the differentiation, maintenance and survival of bacteroids, for nitrogen fixation and for avoidance of early senescence. Given the huge number of NCRs, and the expected redundancy in function of many of these proteins, it was a surprise to find a single NCR with an indispensable role.

NCR169 Is Essential and Unique. *NCR169* is expressed in the transition and nitrogen fixing zones and apparently no other *NCRs* expressed in these zones can fulfill the role of this peptide in its absence. Although *NCR* genes are scattered on the eight chromosomes of *M. truncatula*, many are found in local clusters, as a result of gene duplications (15). This is not the case for *NCR169* (*Medtr7g029760*) as the closest *NCR* genes, *Medtr7g037690* encoding NCR348 and a potential *NCR* (*Medtr7g039150*) are more than 300 kbp away. A similarity search using the *M. truncatula* cv. Jemalong NCR169 identified close homologs in *M. truncatula* ssp. *tricycla* R108 and *M. sativa* with 100% sequence identity of the mature peptides and a homolog in *M. albus* (68% sequence identity of the mature peptides). In *M. truncatula* cv. Jemalong the protein most similar to NCR169 is NCR024 (Medtr5g063460) with 45% identity and 60% similarity between the mature peptides. However, NCR024 is anionic (pI = 4.03) whereas NCR169 is cationic (pI = 8.45), which makes it unlikely that they share a common function.

Although the two mutants, *dnf7* and *dnf4* seem to have very similar phenotype, the NCR169 and NCR211 peptides have distinct, nonredundant functions in the symbiosis. This statement is supported by the different isoelectric point of the peptides and the only partially overlapping expression patterns of the two genes; with *NCR211* being activated earlier and silenced faster than *NCR169*. Importantly, expression of *NCR211* in *dnf7-2* or of *NCR169* in *dnf4* did not restore the WT symbiotic phenotype to either mutant.

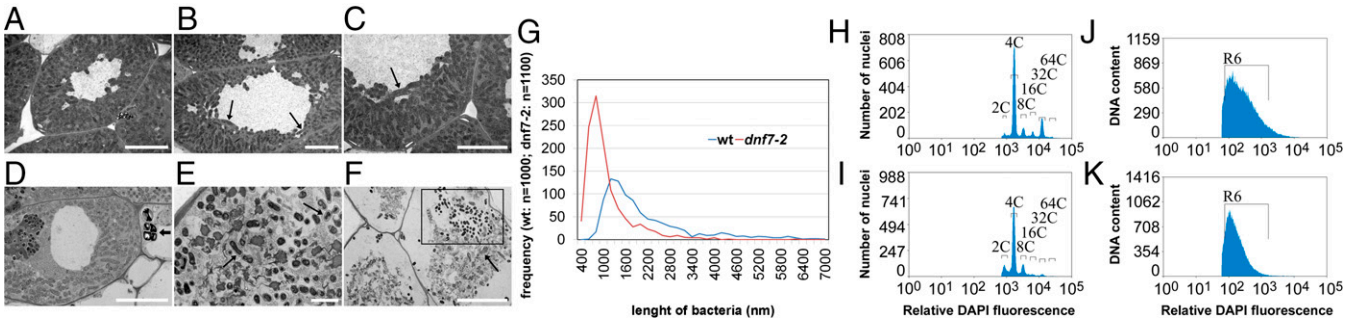

Fig. 3. Symbiotic cells in *dnf7-2* nodules show incomplete differentiation. Electron micrographs display nodule cells with elongated bacteroids in the transition (*A*), distal (*B*) and proximal parts of the nitrogen-fixation zone (*C*) of WT nodules. In the *dnf7-2* nodules, elongation of bacteroids occurs in the transition zone (*D*) but disintegration of the bacteroids and the host cells was observed in the regions of the mutant nodules corresponding to the younger (*E*) and older cells (*F*) of the nitrogen fixation zone in WT nodules. Arrow in *D*: starch granules in the transition zone of mutant nodules (*D*); arrows in *B*, *C*, *E*, and *F* point to symbiosomes with normal (*B* and *C*) and enlarged (*E* and *F*) peribacteroid space in WT (*B* and *C*) and mutant cells (*E* and *F*); bacteria within the rectangle in *F* are liberated from disintegrated infection thread. (Scale bars: 10 μm in *A–D* and *F* and 2 μm in *E*.) (*G*) The distribution of bacteroid size measured in electron micrographs of interzone cells of WT and mutant nodules. The DNA content of plant cells of mutant (*I*) nodules at 16 dpi shifted to lower ploidy level compared with WT cells (*H*). The population of *S. medicae* WSM419 bacteroids with higher DNA content is reduced in *dnf7-2* nodules (*K*) compared with WT samples (*J*).

Inoculation of *dnf7-2* with either *S. meliloti* 1021 or *S. medicae* WSM419 provoked similar mutant phenotypes. Close homologs of NCR169 exist not only in *Medicago* species but also in *M. albus* which is another plant host of the two *Sinorhizobium* species. In contrast, no NCR169 homologs were found in the genomes of *Pisum* and *Trifolium*, which are closely related to *Medicago* but instead of *Sinorhizobium* species they interact with *Rhizobium leguminosarum* bv. *viciae* and bv. *trifolii*, respectively. One possibility is that NCR169 may have specific targets in *S. meliloti* and *S. medicae* but not in other rhizobia, and therefore its function in other legumes is dispensable. However, it cannot be excluded that peptides with unrelated sequence but similar conformation and charge may possess equivalent biological functions in other plants. Moreover, *NCR* genes are not only induced in successive waves (30) but are differentially expressed in *M. truncatula* accessions inoculated with different rhizobial strains (35). The absolute requirement for NCR169 and NCR211 in symbiotic nitrogen fixation with different *Sinorhizobium* strains might suggest the requirement of a core set of NCRs for effective symbiosis; the existence of a pool of differentially expressed NCRs may provide strain specificity or adaptability to different environmental conditions. Existence of such plant and endosymbiont-specific NCR peptides could add a further level of control to host range determination.

NCR Peptide Actions. The in planta functions of NCRs has not yet been reported, although in vitro effect of synthetic cationic NCR peptides have been described (17, 20, 21, 29). NCRs have highly different amino acid compositions, sequences and charges (cationic, neutral or anionic pI), all of which point to different biochemical properties and interactions with the bacterial partners. There is one common characteristic feature of all NCR peptides, the presence of four or six cysteine residues at conserved positions. Substitutions of the four conserved cysteines for serines via chemical synthesis of the NCR247 peptide resulted in a decrease but not complete loss of its in vitro antimicrobial activity (29). In planta, the replacement of individual or multiple cysteines with serine rendered NCR169 unable to complement the *dnf7* mutant. This observation demonstrates that all cysteines are essential for the symbiotic function of NCR169, presumably because they stabilize the 3D structure of the peptide via disulfide bridges. The remaining partial in vitro antimicrobial activity of synthetic NCR247 with replacement of cysteines to serines may be explained by the unchanged high cationic charge of the peptide, which presumably enables the peptide to interact with the bacterial membranes and lyse bacteria at nonphysiological concentrations. Based on its expression pattern, NCR169 probably starts functioning in the transition zone where bacteroids are already partially elongated. In contrast, NCR035 and NCR247 appear to act earlier, when bacterial multiplication is arrested and elongation of bacteroids begins (16, 17). NCR247 binds to the FtsZ bacterial cell division protein and abolishes Z-ring formation whereas NCR035 interacts with the septum (17). It was shown that arrest of cell division by NCR247 was coupled to bacterial enlargement (17). Thus, both peptides, acting on different steps of the same pathway, contribute to inhibition of bacterial cell division. These results suggest that the host targets specific pathways, molecular, metabolic and physiological processes at multiple points with various NCRs to prevent the escape of endosymbionts from plant-controlled differentiation. The role of anionic and neutral NCRs is presently unknown. Nevertheless, the large majority of NCRs identified in isolated bacteroids are anionic and neutral peptides suggesting that they might be the major activators of bacteroid differentiation (18). We do not know how they enter the bacteroids or whether their interaction with cationic peptides helps their penetration. The NCR169-GFP and the NCR169-mCherry fusion proteins seemed to be localized around but not inside the bacteroids. However, we cannot resolve whether a small portion of the fusion proteins or free peptides liberated by the cleavage of the fluorescent tag could enter the rhizobial cells to induce bacteroid development, and so the precise site of the action of NCR169 in bacteroids remains to be determined.

Because pull down experiments demonstrated that NCR247 interact with other NCR peptides (17), it is possible that different cationic, neutral and anionic NCR peptides may act together in complexes. Testing this will require extensive studies to reveal interacting bacterial and plant partners of the various peptides and testing their individual and combined roles.

The similarities in the phenotype of *ncr* mutants but differences in peptide characteristics also indicate that bacteroid development might involve both successive and parallel steps affected by different (complexes of) NCR molecules; failure at any step could conceivably arrest further progress and lead to early nodule senescence.

How can the roles of additional NCRs be characterized in future? Crucial roles for NCR169 and NCR211 were identified via forward genetics. However, this is an untargeted way to characterize further NCRs. Although NCR169 and NCR211 have different isoelectric points, they have four Cys residues in conserved positions and both were abundant in the proteome of bacteroids (18). Such features could be used to select additional NCRs for functional analysis via reverse genetics, using existing mutant populations (37) or via genome editing (38).

Materials and Methods

Bacterial Strains, Plant Material, Growth Conditions, Inoculation, and Nucleic Acid Isolation. Rhizobial strains *S. meliloti* 1021 and *S. medicae* WSM419 containing the P*nifH::uidA* or P*hemA::lacZ* fusions (24) were used for inoculation. *M. truncatula* Jemalong line was used as wild-type (WT) control in all experiments. Wild-type and *dnf7-2* plants were grown and inoculated with bacteria as described in ref. 22. except for transcriptome analysis. FN893-2 and FN9233 were isolated from a deletion mutant collection of *M. truncatula* cv. Jemalong described in ref. 39. For time-course experiments RNA was extracted from roots or nodulated roots, while for gene expression analysis of mutants nodules were harvested at 14 dpi. For transcriptome analysis plants were grown in aeroponic caissons as described in the *Medicago truncatula* Handbook (www.noble.org/MedicagoHandbook). Genomic DNA isolation for genetic mapping, RNA preparation and cDNA synthesis for the gene expression analyses were performed as described in refs. 22 and 40.

Microarray Hybridizations. To identify deletions in the *dnf7-2* genome the Affymetrix GeneChip hybridization was performed as described (25). Genome tiling array-based comparative genomic hybridization (CGH) was carried out according to the manufacturer's protocol (www.genomics.agilent.com/en/home.jsp).

Flow Cytometry. The measurement of DNA content with flow cytometer was carried out as described (41).

SI Materials and Methods describe the details of *M. truncatula* transformation, microscopy, RNA sequencing, data analysis, and qRT-PCR. Table S3 shows primers used in this study.

ACKNOWLEDGMENTS. We thank Allan Downie for critical reading of the manuscript and Istvánné Szívós, Krisztina Miró, and Gábor Halász for skillful technical assistance. The flow cytometer analysis has been carried out at IMAGIF (www.imagif.cnrs.fr) and benefited from the expertise of Mickael Bourge. This work was supported by European Research Council Grant 269067 "Sym-Biotics" (to É.K.); and the Országos Tudományos Kutatási Alapok Grants 67576 (to P.K.), NK105852/106068 (to É.K., A.K., and P.K.), and PD104334/PD108923 (to Á.D.), the bilateral Hungarian-French collaborative program (TÉT_10-1-2011-0397 to A.K. and P.K.), and National Science Foundation Grant Integrative Organismal Systems 1127155 (to M.K.U. and R.C.).

1. Udvardi M, Poole PS (2013) Transport and metabolism in legume-rhizobia symbioses. *Annu Rev Plant Biol* 64:781–805.
2. Oldroyd GED, Downie JA (2008) Coordinating nodule morphogenesis with rhizobial infection in legumes. *Annu Rev Plant Biol* 59:519–546.
3. Vinardell JM, et al. (2003) Endoreduplication mediated by the anaphase-promoting complex activator CCS52A is required for symbiotic cell differentiation in *Medicago truncatula* nodules. *Plant Cell* 15(9):2093–2105.
4. Kondorosi E, Mergaert P, Kereszt A (2013) A paradigm for endosymbiotic life: cell differentiation of Rhizobium bacteria provoked by host plant factors. *Annu Rev Microbiol* 67:611–628.
5. Vasse J, de Billy F, Camut S, Truchet G (1990) Correlation between ultrastructural differentiation of bacteroids and nitrogen fixation in alfalfa nodules. *J Bacteriol* 172(8):4295–4306.
6. Gavrin A, et al. (2014) Adjustment of host cells for accommodation of symbiotic bacteria: vacuole defunctionalization, HOPS suppression, and TIP1g retargeting in *Medicago*. *Plant Cell* 26(9):3809–3822.
7. Mergaert P, et al. (2006) Eukaryotic control on bacterial cell cycle and differentiation in the Rhizobium-legume symbiosis. *Proc Natl Acad Sci USA* 103(13):5230–5235.
8. Scheres B, et al. (1990) Sequential induction of nodulin gene expression in the developing pea nodule. *Plant Cell* 2(8):687–700.
9. Frühling M, et al. (2000) A small gene family of broad bean codes for late nodulins containing conserved cysteine clusters. *Plant Sci* 152(1):67–77.
10. Fedorova M, et al. (2002) Genome-wide identification of nodule-specific transcripts in the model legume *Medicago truncatula*. *Plant Physiol* 130(2):519–537.
11. Kaijalainen S, Schroda M, Lindström K (2002) Cloning of nodule-specific cDNAs of *Galega orientalis*. *Physiol Plant* 114(4):588–593.
12. Mergaert P, et al. (2003) A novel family in *Medicago truncatula* consisting of more than 300 nodule-specific genes coding for small, secreted polypeptides with conserved cysteine motifs. *Plant Physiol* 132(1):161–173.
13. Zhou P, et al. (2013) Detecting small plant peptides using SPADA (Small Peptide Alignment Discovery Application). *BMC Bioinformatics* 14:335.
14. Wang D, et al. (2010) A nodule-specific protein secretory pathway required for nitrogen-fixing symbiosis. *Science* 327(5969):1126–1129.
15. Alunni B, et al. (2007) Genomic organization and evolutionary insights on GRP and NCR genes, two large nodule-specific gene families in *Medicago truncatula*. *Mol Plant Microbe Interact* 20(9):1138–1148.
16. Van de Velde W, et al. (2010) Plant peptides govern terminal differentiation of bacteria in symbiosis. *Science* 327(5969):1122–1126.
17. Farkas A, et al. (2014) *Medicago truncatula* symbiotic peptide NCR247 contributes to bacteroid differentiation through multiple mechanisms. *Proc Natl Acad Sci USA* 111(14):5183–5188.
18. Durgo H, et al. (2015) Identification of nodule-specific cysteine-rich plant peptides in endosymbiotic bacteria. *Proteomics* 15(13):2291–2295.
19. Tiricz H, et al. (2013) Antimicrobial nodule-specific cysteine-rich peptides induce membrane depolarization-associated changes in the transcriptome of *Sinorhizobium meliloti*. *Appl Environ Microbiol* 79(21):6737–6746.
20. Ordögh L, Vörös A, Nagy I, Kondorosi E, Kereszt A (2014) Symbiotic plant peptides eliminate *Candida albicans* both *in vitro* and in an epithelial infection model and inhibit the proliferation of immortalized human cells. *BioMed Res Int* 2014:320796.
21. Penterman J, et al. (2014) Host plant peptides elicit a transcriptional response to control the *Sinorhizobium meliloti* cell cycle during symbiosis. *Proc Natl Acad Sci USA* 111(9):3561–3566.
22. Domonkos A, et al. (2013) The identification of novel loci required for appropriate nodule development in *Medicago truncatula*. *BMC Plant Biol* 13:157.
23. Terpolilli JJ, O'Hara GW, Tiwari RP, Dilworth MJ, Howieson JG (2008) The model legume *Medicago truncatula* A17 is poorly matched for N2 fixation with the sequenced microsymbiont *Sinorhizobium meliloti* 1021. *New Phytol* 179(1):62–66.
24. Starker CG, Parra-Colmenares AL, Smith L, Mitra RM, Long SR (2006) Nitrogen fixation mutants of *Medicago truncatula* fail to support plant and bacterial symbiotic gene expression. *Plant Physiol* 140(2):671–680.
25. Murray JD, et al. (2011) *Vapyrin*, a gene essential for intracellular progression of arbuscular mycorrhizal symbiosis, is also essential for infection by rhizobia in the nodule symbiosis of *Medicago truncatula*. *Plant J* 65(2):244–252.
26. Tang H, et al. (2014) An improved genome release (version Mt4.0) for the model legume *Medicago truncatula*. *BMC Genomics* 15:312.
27. Benedito VA, et al. (2008) A gene expression atlas of the model legume *Medicago truncatula*. *Plant J* 55(3):504–513.
28. Petersen TN, Brunak S, von Heijne G, Nielsen H (2011) SignalP 4.0: discriminating signal peptides from transmembrane regions. *Nat Methods* 8(10):785–786.
29. Haag AF, et al. (2012) Role of cysteine residues and disulfide bonds in the activity of a legume root nodule-specific, cysteine-rich peptide. *J Biol Chem* 287(14):10791–10798.
30. Guefrachi I, et al. (2014) Extreme specificity of *NCR* gene expression in *Medicago truncatula*. *BMC Genomics* 15:712.
31. Roux B, et al. (2014) An integrated analysis of plant and bacterial gene expression in symbiotic root nodules using laser-capture microdissection coupled to RNA sequencing. *Plant J* 77(6):817–837.
32. Maunoury N, et al. (2010) Differentiation of symbiotic cells and endosymbionts in *Medicago truncatula* nodulation are coupled to two transcriptome-switches. *PLoS One* 5(3):e9519.
33. Mitra RM, Long SR (2004) Plant and bacterial symbiotic mutants define three transcriptionally distinct stages in the development of the *Medicago truncatula/Sinorhizobium meliloti* symbiosis. *Plant Physiol* 134(2):595–604.
34. Ding Y, et al. (2008) Abscisic acid coordinates nod factor and cytokinin signaling during the regulation of nodulation in *Medicago truncatula*. *Plant Cell* 20(10):2681–2695.
35. Nallu S, et al. (2013) Regulatory patterns of a large family of defensin-like genes expressed in nodules of *Medicago truncatula*. *PLoS One* 8(4):e60355.
36. Pérez Guerra JC, et al. (2010) Comparison of developmental and stress-induced nodule senescence in *Medicago truncatula*. *Plant Physiol* 152(3):1574–1584.
37. Tadege M, et al. (2008) Large-scale insertional mutagenesis using the *Tnt1* retrotransposon in the model legume *Medicago truncatula*. *Plant J* 54(2):335–347.
38. Belhaj K, Chaparro-Garcia A, Kamoun S, Nekrasov V (2013) Plant genome editing made easy: targeted mutagenesis in model and crop plants using the CRISPR/Cas system. *Plant Methods* 9(1):39.
39. Xi J, Chen Y, Nakashima J, Wang SM, Chen R (2013) *Medicago truncatula esn1* defines a genetic locus involved in nodule senescence and symbiotic nitrogen fixation. *Mol Plant Microbe Interact* 26(8):893–902.
40. Horváth B, et al. (2011) *Medicago truncatula* IPD3 is a member of the common symbiotic signaling pathway required for rhizobial and mycorrhizal symbioses. *Mol Plant Microbe Interact* 24(11):1345–1358.
41. Sinharoy S, et al. (2013) The C_2H_2 transcription factor regulator of symbiosome differentiation represses transcription of the secretory pathway gene *VAMP721a* and promotes symbiosome development in *Medicago truncatula*. *Plant Cell* 25(9):3584–3601.
42. Boivin C, Camut S, Malpica CA, Truchet G, Rosenberg C (1990) *Rhizobium meliloti* genes encoding catabolism of trigonelline are induced under symbiotic conditions. *Plant Cell* 2(12):1157–1170.
43. Haag AF, et al. (2011) Protection of Sinorhizobium against host cysteine-rich antimicrobial peptides is critical for symbiosis. *PLoS Biol* 9(10):e1001169.
44. Boisson-Dernier A, et al. (2001) *Agrobacterium rhizogenes*-transformed roots of Medicago truncatula for the study of nitrogen-fixing and endomycorrhizal symbiotic associations. *Mol Plant Microbe Interact* 14(6):695–700.
45. Anders S, Huber W (2010) Differential expression analysis for sequence count data. *Genome Biol* 11(10):R106.